Available online at www.sciencedirect.com

ScienceDirect

IFAC PapersOnline CONFERENCE PAPER ARCHIVE

IFAC PapersOnLine 51-29 (2018) 116–121

Development of a Dynamic Positioning System for the ReVolt Model Ship

Henrik Lemcke Alfheim * **Kjetil Muggerud** * **Morten Breivik** *
Edmund Førland Brekke * **Egil Eide** **
Øystein Engelhardtsen ***

* *Department of Engineering Cybernetics, Norwegian University of Science and Technology (NTNU), NO-7491, Trondheim, Norway (e-mail: henrik.alfheim@gmail.com, muggeru@gmail.com, morten.breivik@ieee.org, edmund.brekke@ntnu.no)*
** *Department of Electronic Systems, Norwegian University of Science and Technology (NTNU), NO-7491, Trondheim, Norway (e-mail: egil.eide@ntnu.no)*
*** *DNV GL, Oslo, Norway (e-mail: oystein.engelhardtsen@dnvgl.com)*

Abstract:
A Dynamic Positioning (DP) control system is developed, implemented and tested for a scale model of DNV GL's concept ship ReVolt. This model-scale ship is used as a test platform for sensors and control systems used in autonomous vessels, and this paper focuses on the functionality and implementation of the components and control system required to achieve DP capabilities on the ReVolt model ship. The DP system consists of a 3-Degree of Freedom reference filter, Proportional-Integral-Derivative (PID) controller with a model-based reference feedforward, and a thrust allocation module from DNV GL. The DP system is implemented on ReVolt's onboard computer, which runs the Robot Operating System (ROS) on top of a Linux shell. Field tests are conducted, with the main objective to achieve station keeping and low-speed maneuvering capabilities for ReVolt. Different setups in the thrust allocation and controller are assessed by performance metrics to determine the best overall setup for ReVolt.

Keywords: Dynamic positioning, Revolt model ship, Robot operating system, rapid prototyping platform, experimental results

1. INTRODUCTION

During the past century, automation has revolutionized numerous industries by replacing manual labor with automated machinery, and in recent years automation has entered our homes in the form of lawn mowers, vacuum cleaners or even the house itself. A shift from automated systems, which specialize on specifically defined technical tasks, to autonomous systems, which are capable of self governing complex tasks without human interaction, is currently emerging.

Autonomous Surface Vehicles (ASVs) are still in the early stages of development and show great potential. Such vessels can be used in different scientific and commercial operations, potentially outperforming manned vessels in safety, endurance and cost efficiency. One such ship is DNV GL's concept ship ReVolt (DNV GL, 2015), which was introduced in 2014. A scale model ship of ReVolt was built and brought to NTNU in 2016 to serve as a test platform for developing control systems for ASVs.

In order to make ReVolt autonomous, the first step is to develop and implement a Dynamic Positioning (DP) control system, which is crucial for low speed maneuvering close to shore and other vessels. This is furthermore the foundation for advanced guidance systems, such as path-following and collision avoidance. For more details about DP, see (Fossen, 2011).

The main contribution of this paper is to develop and implement a 3-Degree of Freedom (DOF) DP control system for ReVolt. The control system consists of a Proportional-Integral-Derivative (PID) controller, model based feedforward and reference filter. The performance with and without feedforward, as well as different constraints in the thruster allocation, is assessed.

This paper can be used as a starting guide for others who would like to create a test platform such as ReVolt. More in-depth information about experiences using the Robot Operating System (ROS), rapid control prototyping or ReVolt can be found in (Alfheim and Muggerud, 2017).

2. MODELING AND CONTROL DESIGN

2.1 Vessel model

From (Fossen, 2011), the 3-DOF marine craft equations of motion is written as:

$$\dot{\boldsymbol{\eta}} = \boldsymbol{R}(\psi)\boldsymbol{\nu} \tag{1}$$

$$\boldsymbol{M}\dot{\boldsymbol{\nu}} + \boldsymbol{C}(\boldsymbol{\nu})\boldsymbol{\nu} + \boldsymbol{D}(\boldsymbol{\nu})\boldsymbol{\nu} = \boldsymbol{\tau}_{thruster} + \boldsymbol{\tau}_{environment} \tag{2}$$

Peer review under responsibility of International Federation of Automatic Control.
10.1016/j.ifacol.2018.09.479

where $\boldsymbol{\eta} \in \mathbb{R}^3$ is the position and heading (pose) vector and $\boldsymbol{\nu} \in \mathbb{R}^3$ is the velocity vector of the vessel. The rotation matrix $\boldsymbol{R}(\psi) \in \mathbb{R}^{3\times3}$ transforms the velocity from the Body-fixed (BODY) to the North-East-Down (NED) reference frame. $\boldsymbol{\tau}_{thruster} \in \mathbb{R}^3$ and $\boldsymbol{\tau}_{environment} \in \mathbb{R}^3$ are the forces and moment vectors of the thrusters and environment on the vessel. The inertia matrix is represented by $\boldsymbol{M} \in \mathbb{R}^{3\times3}$, which is the sum of rigid-body inertia matrix $\boldsymbol{M}_{RB} \in \mathbb{R}^{3\times3}$ and hydrodynamic added mass $\boldsymbol{M}_A \in \mathbb{R}^{3\times3}$. The matrix $\boldsymbol{C}(\boldsymbol{\nu}) \in \mathbb{R}^{3\times3}$ consists of the Coriolis and Centripetal terms, while $\boldsymbol{D}(\boldsymbol{\nu}) \in \mathbb{R}^{3\times3}$ consists of the damping forces which usually are modelled as a sum of constants and some velocity dependent terms. For a vessel operating around zero speed, it is reasonable to assume that linear damping will dominate over non-linear damping.

2.2 Reference Filter

A reference filter is used to generate a suitable trajectory the vessel can follow. For big changes in setpoint, the controller will act on a big error which in most cases will lead to a sudden huge demand in control effort. This may then generate unwanted behavior from the vessel. In order to generate a suitable trajectory for position and attitude, a third order linear reference filter is chosen. The reference filter is defined as stated in (Fossen, 2011):

$$\dddot{\boldsymbol{\eta}}_d + (2\boldsymbol{\Delta}+\mathbf{I})\boldsymbol{\Omega}\ddot{\boldsymbol{\eta}}_d + (2\boldsymbol{\Delta}+\mathbf{I})\boldsymbol{\Omega}^2\dot{\boldsymbol{\eta}}_d + \boldsymbol{\Omega}^3\boldsymbol{\eta}_d = \boldsymbol{\Omega}^3\boldsymbol{\eta}_{\text{ref}} \quad (3)$$

where $\boldsymbol{\eta}_d \in \mathbb{R}^3$ is the desired pose, given in the NED frame. The input to the filter is $\boldsymbol{\eta}_{\text{ref}} \in \mathbb{R}^3$ and is given in the NED frame. The output $\boldsymbol{\eta}_d$ and the input $\boldsymbol{\eta}_{\text{ref}}$ are given by:

$$\boldsymbol{\eta}_d = \begin{bmatrix} N_d \\ E_d \\ \psi_d \end{bmatrix} \qquad \boldsymbol{\eta}_{\text{ref}} = \begin{bmatrix} N_{\text{ref}} \\ E_{\text{ref}} \\ \psi_{\text{ref}} \end{bmatrix} \quad (4)$$

The diagonal matrix $\boldsymbol{\Delta} > 0$, contains the relative damping ratios, $\zeta_i, i = 1, 2, 3$, and $\boldsymbol{\Omega} > 0$ is a diagonal matrix with the natural frequencies ω_i, where $i \in 1, 2, 3$.

The continuous-time equation for the reference filter in (3) can be written in the state-space form:

$$\dot{\boldsymbol{x}} = \boldsymbol{A}\boldsymbol{x} + \boldsymbol{B}\boldsymbol{u} \quad (5)$$

as

$$\begin{bmatrix} \dot{\boldsymbol{\eta}}_d \\ \ddot{\boldsymbol{\eta}}_d \\ \dddot{\boldsymbol{\eta}}_d \end{bmatrix} = \begin{bmatrix} 0 & \mathbf{I} & 0 \\ 0 & 0 & \mathbf{I} \\ -\boldsymbol{\Omega}^3 & -\boldsymbol{G}\boldsymbol{\Omega}^2 & -\boldsymbol{G}\boldsymbol{\Omega} \end{bmatrix} \begin{bmatrix} \boldsymbol{\eta}_d \\ \dot{\boldsymbol{\eta}}_d \\ \ddot{\boldsymbol{\eta}}_d \end{bmatrix} + \begin{bmatrix} 0 \\ 0 \\ \boldsymbol{\Omega}^3 \end{bmatrix} \boldsymbol{\eta}^n_{\text{ref}} \quad (6)$$

where $\boldsymbol{G} = 2\boldsymbol{\Delta} + \mathbf{I}$.

2.3 PID controller with Feedforward

There are several types of controllers that can be used for DP, ranging from simple controllers to more advanced ones. Examples of simple controllers are the PID controller, which is a robust and industry standard feedback controller used in many applications, and the Linear Quadratic Regulator (LQR), which is based on a mathematical model of the vessel, while adaptive backstepping (Sørensen et al., 2016) is an example of a more advanced controller. The PID controller is chosen for the feedback part. To aid the PID with setpoint changes, a feedforward term utilizing a vessel model obtained from simulations is added. The total control law is then written:

$$\boldsymbol{\tau} = \boldsymbol{\tau}_{FF} + \boldsymbol{\tau}_{PID} \quad (7)$$

When using a PID controller in a DP control system, it is common that the desired setpoint is in 3 DOF. This is achieved using $\boldsymbol{\eta}^b \in \mathbb{R}^3$, where

$$\boldsymbol{\eta}^b = \boldsymbol{R}(\psi)^\intercal \boldsymbol{\eta} \quad (8)$$

which gives the continuous-time PID equation:

$$\boldsymbol{\tau}_{PID}(t) = -\mathbf{K}_P\boldsymbol{\eta}^b_{error}(t) - \mathbf{K}_I \int_0^t \boldsymbol{\eta}^b_{error}(\tau)d\tau - \mathbf{K}_D\dot{\boldsymbol{\eta}}^{\boldsymbol{b}}_{\boldsymbol{error}}(\boldsymbol{t}) \quad (9)$$

where

$$\boldsymbol{\eta}^b_{error} = \boldsymbol{\eta}^b - \boldsymbol{\eta}^b_d \quad (10)$$

To implement a PID controller, the continuous-time PID control equation (9) is discretized using implicit Euler method (Fossen, 2011), giving the following feedback control law:

$$\boldsymbol{\tau}_{PID}(h) = -\mathbf{K}_P\boldsymbol{\eta}^b_{error}(h) - \mathbf{K}_I \sum_{i=0}^{i} \boldsymbol{\eta}^b_{error}(i)h - \mathbf{K}_D\frac{1}{h}\boldsymbol{\nu}_{error}(h) \quad (11)$$

where

$$\boldsymbol{\nu}_{error} = \boldsymbol{\nu} - \boldsymbol{\nu}_d \quad (12)$$

and $\boldsymbol{\nu}_d \in \mathbb{R}^3$ denotes the desired velocity. The timestep in the controller is given by h.

A simple anti-windup and control saturation is implemented to prevent integration wind-up in the PID controller.

In the controller, a model-based reference feedforward is used, based on the model in (2). The model-based feedforward calculates necessary forces to obtain the desired changes in setpoint, based on the vessel model, and forward these into the control system. For a good model, this leaves the PID controller dealing only with environmental forces and not setpoint changes. The feedforward term becomes:

$$\boldsymbol{\tau}_{FF} = \boldsymbol{M}\dot{\boldsymbol{\nu}}_{\boldsymbol{d}} + \boldsymbol{C}(\boldsymbol{\nu})\boldsymbol{\nu}_d + \boldsymbol{D}(\boldsymbol{\nu})\boldsymbol{\nu}_d \quad (13)$$

where $\dot{\boldsymbol{\nu}}_{\boldsymbol{d}} \in \mathbb{R}^3$ denotes the desired accelerations.

When implementing the feedforward term in a practical system, $\boldsymbol{C}(\boldsymbol{\nu}_d)$, $\boldsymbol{D}(\boldsymbol{\nu}_d)$ and $\dot{\boldsymbol{\nu}}_d$ are used instead of $\boldsymbol{C}(\boldsymbol{\nu})$, $\boldsymbol{D}(\boldsymbol{\nu})$ and $\dot{\boldsymbol{\nu}}$. This is because the desired setpoints are a much more stable signal than the system states signal. If the state signal becomes corrupted or is estimated incorrectly, the entire system can become unstable. Hence the feedforward term in (7) is chosen as:

$$\boldsymbol{\tau}_{FF} = \boldsymbol{M}\dot{\boldsymbol{\nu}}_{\boldsymbol{d}} + \boldsymbol{C}(\boldsymbol{\nu}_d)\boldsymbol{\nu}_d + \boldsymbol{D}(\boldsymbol{\nu}_d)\boldsymbol{\nu}_d \quad (14)$$

2.4 Thrust Allocation

Actuators can exert forces and moments on the ship and are used by the DP system to control the ship pose and velocity. How well the DP system's commanded forces

are realized depends greatly on each actuator and their position on the vessel relative to Center of Gravity (CG), as well as the Thrust Allocation (TA) ability to handle the thruster's dynamics.

The relationship between the propeller thrust F and the shaft speed n at zero speed, is given by: (Sørensen, 2013)

$$F = sign(n)K_T\rho D^4 n^2 \tag{15}$$

where D is the propeller diameter and ρ is the water density. The thrust coefficient $K_T > 0$ is usually found by performing a bollard pull test where the force applied to the vessel by the propeller is measured. In some cases, n is not the input to the thruster, thus a simplified model using the control input is written as a linear model: (Fossen, 2011)

$$\boldsymbol{F} = \boldsymbol{K}\boldsymbol{u} \tag{16}$$

where $\boldsymbol{F} \in \mathbb{R}^r$ (r = 3, number of thrusters) is the generated force by the thrusters, $\boldsymbol{K} \in \mathbb{R}^{r\times r}$ is the new force coefficient, and $\boldsymbol{u} \in \mathbb{R}^r$ is the control input to the thruster. The force exerted from the thrusters can then be measured at different control inputs, and by using linear regression the force coefficients are found.

2.5 Thrust Configuration Matrix

To find the forces and moments the thrusters exert on the vessel $\boldsymbol{\tau} \in \mathbb{R}^n$, a thrust configuration matrix is set up. For this, the CG is assumed to be known and defined, as well as every thruster's position with respect to this point. The forces and moments applied to the vessel are now defined by:

$$\boldsymbol{\tau} = \boldsymbol{T}(\boldsymbol{\alpha})\boldsymbol{F} \tag{17}$$

where $\boldsymbol{\alpha} \in \mathbb{R}^r$ is a vector of azimuth angles and $\boldsymbol{T}(\boldsymbol{\alpha}) \in \mathbb{R}^{n\times r}$ is the thrust configuration matrix. By inserting (16) into (17) we get:

$$\boldsymbol{\tau} = \boldsymbol{T}(\boldsymbol{\alpha})\boldsymbol{K}\boldsymbol{u} \tag{18}$$

For a 3-DOF system with the thruster geometry presented in Figure 2, the dimensions become: $\boldsymbol{\tau} \in \mathbb{R}^3$, $\boldsymbol{u} \in \mathbb{R}^3$, and $\boldsymbol{T}(\boldsymbol{\alpha}) \in \mathbb{R}^{3\times 3}$. The thrust configuration matrix then becomes:

$$\boldsymbol{T}(\boldsymbol{\alpha}) = \begin{bmatrix} c(\alpha_1) & c(\alpha_2) & c(\alpha_3) \\ s(\alpha_1) & s(\alpha_2) & s(\alpha_3) \\ l_{x1}s(\alpha_1) & l_{y2}c(\alpha_2) - l_{x2}s(\alpha_2) & l_{y3}c(\alpha_3) - l_{x3}s(\alpha_3) \end{bmatrix} \tag{19}$$

where $s = sin$ and $c = cos$.

The control input and azimuth angles are now:

$$\boldsymbol{u} = [u_1 \ u_2 \ u_3]^\mathsf{T} \qquad \boldsymbol{\alpha} = [\alpha_1 \ \alpha_2 \ \alpha_3]^\mathsf{T} \tag{20}$$

3. HARDWARE PLATFORM

ReVolt, shown in Figure 1, is fitted with 3 actuators, two at the stern and one in the bow. The overall length is 3.00 m and the width is 0.72 m. The weight of ReVolt is 257 kg, including weights which are added for stability purposes. ReVolt has a top speed of approximately 2 knots, with a maximum combined engine power of 360 W.

The two identical stern thrusters consist of an AC-motor to drive the propeller, which are powered by an Electronic Speed Controller (ESC) rated at 40 A. The pod is rotated

Fig. 1. The model-scale ship ReVolt under way at Havnebasseng VI in Trondheim.

by a stepper motor via a belt system, allowing for indefinite rotation of the stern thrusters. The stepper motors are of the type Nanotec PD2-N41 motor, which have an RS485 interface. The stepper motors use an encoder to ensure closed-loop position control, which is tuned and set up via the manufacturer's program called NanoPro.

The bow thruster consists of a DC-motor to rotate the propeller, which is powered by an ESC rated at 35 A. The propeller house is rotated by a servo motor, which is capable of rotating ± 270°. A linear actuator is mounted to both a construction that holds the DC-motor and a servo, enabling the propeller house to be lowered or retracted in and out of the vessel's hull.

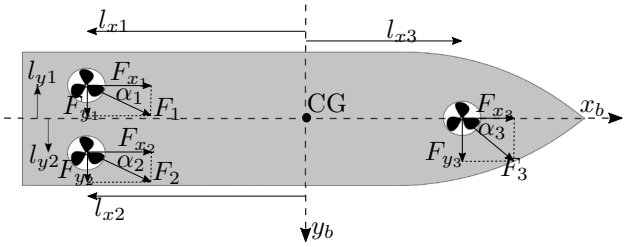

Fig. 2. The thruster configuration for ReVolt, decomposed along the body x- and y-axis. Here, $l_x1 = l_{x2} = 1.12$ m, $l_{x3} = 1.08$ m, $l_{y1} = l_{y2} = 0.15$ m

A Vector VS330 dual antenna Global Navigation Satellite System (GNSS) receiver is used to measure ReVolt's position and heading. Using the two antennas, the Vector measures the heading, which is stabilized with an internal gyro. This is called a GNSS-compass. It also supports different correction data, such as SBAS and RTK, improving the accuracy and precision of the position measurements. The antennas are mounted with the forward antenna as the primary and a baseline of 2.05 m along the centerline of the vessel.

With Real-Time Kinematic (RTK) correction data, the Vector VS330 is able to provide accurate heading and position measurement down to ±0.2° and ±1 cm, according to the Vector VS330 data sheet.

4. SOFTWARE PLATFORM

The entire control system is created on a software framework called Robot Operating System (ROS), which is a collection of open-source software libraries. These provide

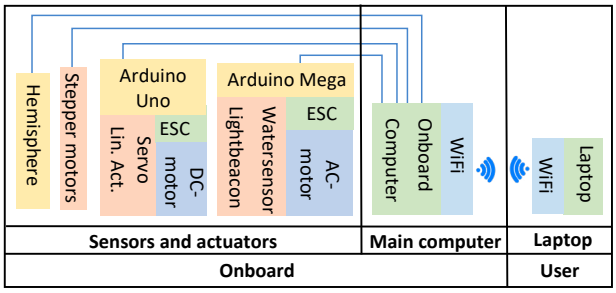

Fig. 3. Revolt system overview. (Lin. Act. = Linear Actuator)

an operating system-like functionality and can be used to create a modular system using nodes. These nodes are executable files which are written in C++ or Python, with support for more programming languages being added. On ReVolt, the ROS distribution ROS Indigo Igloo was used (Marguedas, 2017).

The roscore is the main hub of the system, functioning as a registration service for other nodes, as well as keeping track of messages enabling nodes to communicate with other nodes. The messages in ROS are called topics and are sent and received by nodes using a TCP/IP-based message transport, called TCPROS. Nodes publish and subscribe to topics, as they are not addressed to a specific node. Nodes written in different languages can communicate using topics as long as the structure of the data in the topic is known for both nodes.

A simple Graphical User Interface (GUI) is developed using a standard package in ROS, which enables easy configuration of parameters in the system, such as the PID controller and switching modes. The GUI can be accessed using a laptop connected to the onboard computer on ReVolt through WiFi. See Figure 3 for a overview of the main components in ReVolt.

DNV GL's TA is implemented on ReVolt, which basically is a constrained quadratic optimization solver. It solves a quadratic programming variant of (17) on $\boldsymbol{\alpha}$, which is used directly, and $\boldsymbol{F}$, which is converted to input $\boldsymbol{u}$. It punishes big steps in control forces while seeking the optimum inputs to attain desired control force. The solver is written in Java, which has been interfaced with ROS. For more details, see (Alfheim and Muggerud, 2017).

5. EXPERIMENTAL SETUP

5.1 Test Scenario - 4-Corner Test

To test the DP system, a 4-corner test used during the AMOS research cruise 2016 (Skjetne et al., 2017) has been adopted. This is shown in Figure 4. The 4-corner box test ensures that most motions of the vessel are tested and it is practical during real life experiments because the vessel returns to the initial position and heading, ready for another test.

The test starts with the vessel pointing north at heading 0° and then the following reference changes are commanded:

(1) Change position x meters due north and come to a complete stop. This tests surge motion ahead.

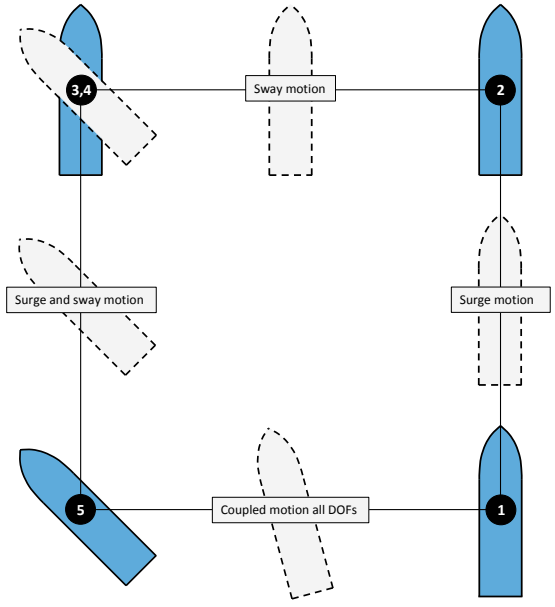

Fig. 4. The 4-corner box test.

(2) Change position x meters due west and come to a complete stop. This tests sway motion to port.
(3) Change heading 45° counterclockwise and come to a complete stop. This tests yaw motion.
(4) Change position x meters due south and come to a complete stop. This tests a coupled sway and surge motion to port and astern, respectively.
(5) Change position x meters due east and change heading 45° clockwise and come to a complete stop. This tests a coupled surge, sway and yaw motion.

5.2 Performance Metrics

To compare controller performance, the errors in position $\boldsymbol{p}$ and heading ψ are normalized between -1 and 1, where it is assumed that the biggest errors are 5m and 50° in north/east position and heading, respectively. This gives the normalized values:

$$\bar{\boldsymbol{p}} = \frac{\boldsymbol{p}}{5}, \quad \bar{\boldsymbol{p}}_d = \frac{\boldsymbol{p}_d}{5}, \quad \bar{\psi} = \frac{\psi}{50}, \quad \bar{\psi}_d = \frac{\psi_d}{50} \tag{21}$$

These normalized values are then integrated over time, giving the equation for calculating the Integrated Absolute Error (IAE), which is given as:

$$IAE(t) = \int_0^t |\bar{e}(\sigma)| d\sigma \tag{22}$$

where $\bar{e}(t)$ is the error at time t and is defined as

$$\bar{e}(t) = \sqrt{(\bar{\boldsymbol{p}}(t) - \bar{\boldsymbol{p}}_d(t))^2 + (\bar{\psi}(t) - \bar{\psi}_d(t))^2)} \tag{23}$$

The Integral of Absolute Differentiated Control (IADC) is adapted from (Eriksen and Breivik, 2017), and is used to assess each scenario's wear and tear on the actuators. The change in actuator input is integrated to get the accumulated difference in actuator input over time. The modified IADC is then given as:

$$IADC(t) = \int_0^t |\dot{\bar{\boldsymbol{u}}}(\sigma)| + |\dot{\bar{\boldsymbol{\alpha}}}(\sigma)| d\sigma \tag{24}$$

where $\dot{\bar{\boldsymbol{u}}}$ and $\dot{\bar{\boldsymbol{\alpha}}}$ are the normalized differences in actuator input at a given time t and are defined as:

$$\dot{\bar{\boldsymbol{u}}}(t) = \frac{\bar{\boldsymbol{u}}(t) - \bar{\boldsymbol{u}}(t-h)}{h}, \qquad \bar{\boldsymbol{u}} = \frac{\boldsymbol{u}}{100} \tag{25}$$

$$\dot{\bar{\boldsymbol{\alpha}}}(t) = \frac{\bar{\boldsymbol{\alpha}}(t) - \bar{\boldsymbol{\alpha}}(t-h)}{h}, \qquad \bar{\boldsymbol{\alpha}} = \frac{\boldsymbol{\alpha}}{90^\circ} \tag{26}$$

where h is the timestep of the controller.

5.3 Bollard Pull Tests

As the propellers used on ReVolt are custom made, there are no available data on the force they generate at certain shaft speeds. As a solution to this, a crude bollard pull test is conducted in calm sea. The test is conducted by tying a rope to the end of the boat and placing a digital luggage scale in the other end. Each type of thrusters are then mapped at different inputs and curve fitting techniques are used to find a suitable constant. The model used is:

$$F_i = K_i |u_i| u_i \tag{27}$$

where the subscript of K_i denotes the thruster number, given in Figure 2.

Due to the bow thruster's asymmetrical propeller design, it does not produce the same thrust in both directions as opposed to the stern thrusters. The constants are thus:

$$\begin{aligned} K_1^{\pm} = K_2^{\pm} = 2.7e-3[N/u^2] \\ K_3^{-} = 6.172e-4[N/u^2] \quad K_3^{+} = 1.518e-3[N/u^2] \end{aligned} \tag{28}$$

With these values implemented in the TA, a map of available thrust for each angle is calculated. The two scenarios: rotatable bow thruster (blue) and fixed bow thruster (red) is presented in Figure 5.

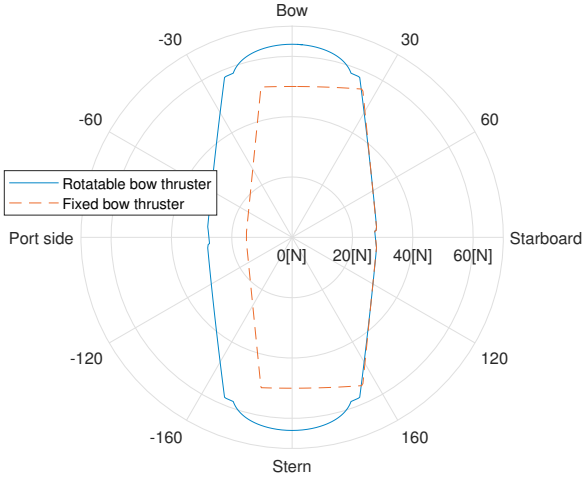

Fig. 5. ReVolt's available thrust for all directions with $F_1^{min} = F_2^{min} = F_1^{max} = F_2^{max} = 25[\text{N}]$, $F_3^{max} = 14[\text{N}]$ and $F_3^{min} = -6.1[\text{N}]$

5.4 Reference Filter Parameters

The reference filter parameters are chosen through simulations and are tuned conservatively such that ReVolt is able to easily follow the desired trajectory generated by the reference filter. The reference filter could be tuned more aggressively, making ReVolt move faster, but this is not the purpose. The following parameters are thus used:

$$\boldsymbol{\Delta} = \begin{bmatrix} \zeta_N \\ \zeta_E \\ \zeta_{psi} \end{bmatrix} = \begin{bmatrix} 1 \\ 1 \\ 1 \end{bmatrix} \quad , \quad \boldsymbol{\Omega} = \begin{bmatrix} \omega_{n,N} \\ \omega_{n,E} \\ \omega_{n,\psi} \end{bmatrix} = \begin{bmatrix} 0.6 \\ 0.6 \\ 0.6 \end{bmatrix} \tag{29}$$

5.5 Controller Gains

The saturation limits in the controller are set according to the maximum thrust the ship's thrusters can supply, as shown in Figure 5. Since the maximum thrust is different for ±sway and ±yaw rotation, a compromise is made and a suitable value is chosen. The saturation limits are:

$$\boldsymbol{\tau}_{max} = \begin{bmatrix} \tau_{X,max} \\ \tau_{Y,max} \\ \tau_{N,max} \end{bmatrix} = \begin{bmatrix} 50 \\ 20 \\ 32 \end{bmatrix} \begin{bmatrix} N \\ N \\ Nm \end{bmatrix} \tag{30}$$

The controller is manually tuned directly on the physical system during the experiments, and the following controller gains are obtained:

$$\boldsymbol{K_p} = \begin{bmatrix} K_{p,surge} & 0 & 0 \\ 0 & K_{p,sway} & 0 \\ 0 & 0 & K_{p,yaw} \end{bmatrix} = \begin{bmatrix} 25 & 0 & 0 \\ 0 & 25 & 0 \\ 0 & 0 & 30 \end{bmatrix} \tag{31}$$

$$\boldsymbol{K_i} = \begin{bmatrix} K_{i,surge} & 0 & 0 \\ 0 & K_{i,sway} & 0 \\ 0 & 0 & K_{i,yaw} \end{bmatrix} = \begin{bmatrix} 0.3 & 0 & 0 \\ 0 & 0.3 & 0 \\ 0 & 0 & 0.3 \end{bmatrix} \tag{32}$$

$$\boldsymbol{K_d} = \begin{bmatrix} K_{d,surge} & 0 & 0 \\ 0 & K_{d,sway} & 0 \\ 0 & 0 & K_{d,yaw} \end{bmatrix} = \begin{bmatrix} 75 & 0 & 0 \\ 0 & 75 & 0 \\ 0 & 0 & 50 \end{bmatrix} \tag{33}$$

6. EXPERIMENTAL RESULTS

To fully test the DP control system and capabilities of ReVolt, a series of 4-corner box tests was conducted in the beginning of May 2017. The tests are held in a calm area behind breakwaters, with a slight north-east breeze and no significant current. The objective of the test is to find the best setup for ReVolt among the following setups: Unconstrained TA (Uncon), Constrained TA (Con), Constrained TA with rotatable bow thruster (Rot), and Constrained TA with feedforward.

During testing, ReVolt's model is found inaccurate, as its performance with feedforward is not one expects. During the test, the controller output quickly reach saturation limits causing Revolt to exceed its velocities obtained from the reference filter, which results in large overshoots in pose. This results in a high IAE value as shown in Figure 6 although it received a low score on the IADC, due to the feedforward saturating the control inputs, thus rendering the PID insufficient.

As shown in the IAE plot at the top in Figure 6, the unconstrained setup managed to follow the desired trajectory best. However, the IADC is substantially higher than the the constrained setups. What is not intuitive is that the setup with rotating bow thruster does not perform among the best in terms of IAE. This can be explained by the poor performance of the bow thruster, resulting in forces exerted in unintended directions. For more details on the actuator performance, see (Alfheim and Muggerud, 2017).

The best result, as shown in Figure 7, is achieved with constrained TA, a static bow thruster and no feedforward.

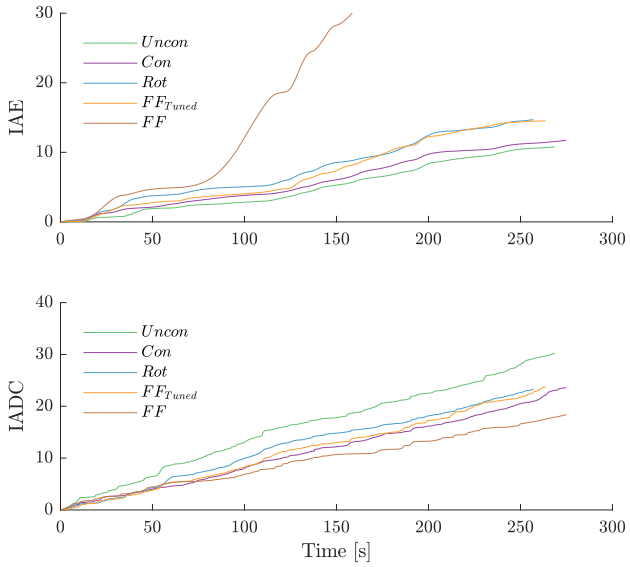

Fig. 6. IAE and IADC results from the different setups from ReVolt's DP control system.

ReVolt is able to follow the desired trajectory with a maximal error of 0.3 m in the north direction, 0.5 m in the east direction and 6.5° in the heading. These errors occur during the coupled surge-sway motion from point 4 to 5 in the 4-corner box test. This coupled maneuver is in itself difficult for ReVolt's control system, especially since the bow thruster produce the least amount of thrust in negative sway. Setting the bow thruster in the opposite direction to -90° may yield a better result for this specific maneuver, but will impair the coupled movement in positive sway direction.

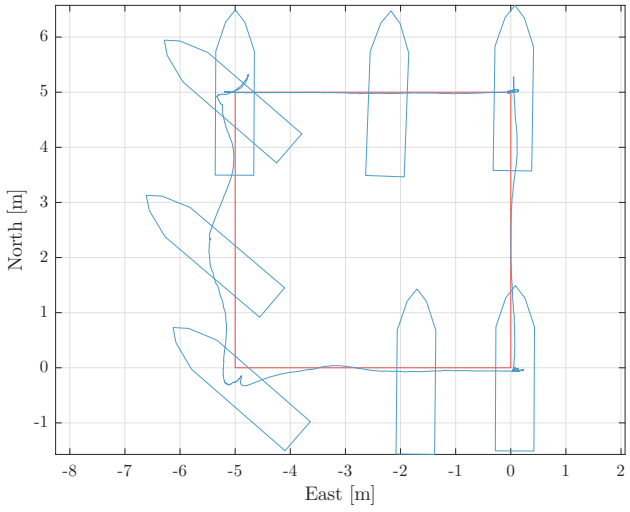

Fig. 7. The best result for the 4-corner box maneuver achieved by ReVolt. The ship outline has the same dimensions as ReVolt.

7. CONCLUSION

The control system of the model ship ReVolt is simulated, implemented, tested and refined. ReVolt is now able to follow a desired trajectory using a GNSS with RTK corrections as the navigational sensor. The ship is also able to achieve station keeping and low-speed maneuvering capabilities, with the best setup being a constrained thrust allocation, a static bow thruster at 90° and with the PID controller. The maximal errors occur during the coupled surge-sway motion, which is especially challenging for ReVolt's control system to perform.

Future work on ReVolt should include improving the mathematical ship model for ReVolt. Experimentally identifying the model would render the feedforward useful and probably improve the performance of ReVolt during maneuvering and can furthermore also be used for more advanced controllers and estimators. Developing way-point tracking and path following capabilities would also improve ReVolt as a test platform. Additional sensors, such as a LIDAR, camera and radar, should be considered implemented to increase ReVolt's situational awareness and to aid in navigation. With such sensors, ReVolt can detect obstacles and the implementation of collision avoidance capabilities can be added to the control system.

8. ACKNOWLEDGEMENTS

This work is partially supported by the Research Council of Norway through projects 223254 (Centre for Autonomous Marine Operations and Systems at NTNU) and 244116 (Sensor Fusion and Collision Avoidance for Autonomous Marine Vehicles), which also are funded by DNV GL, Kongsberg Maritime and Maritime Robotics.

REFERENCES

Alfheim, H.L. and Muggerud, K. (2017). *Development of a Dynamic Positioning System for the ReVolt Model Ship*. Master's thesis, Norwegian University of Science and Technology, Trondheim, Norway.

DNV GL (2015). ReVolt main report. Technical Report 2015-0170, Rev.1, DNV GL, Høvik, Norway.

Eriksen, B.H. and Breivik, M. (2017). *Modeling, Identification and Control of High-Speed ASVs: Theory and Experiments*, 407–431. Springer International Publishing, Cham.

Fossen, T.I. (2011). *Handbook of Marine Craft Hydrodynamics and Motion Control*. John Wiley & Sons.

Marguedas (2017). ROS distributions. http://wiki.ros.org/Distributions. URL `http://wiki.ros.org/Distributions`. Last Accessed: 06 June 2018.

Skjetne, R., Sørensen, M.E.N., Breivik, M., Sørensen, A.J., Brodtkorb, A.H., Værnø, S.A.T., Kjerstad, Ø.K., Vinje, B.O., and Calabrò, V. (2017). AMOS DP research cruise 2016: Academic full-scale testing of experimental dynamic positioning control algorithms onboard R/V gunnerus. In *Proceedings of OMAE, Trondheim, Norway, June 2017*.

Sørensen, A.J. (2013). Marine control systems propulsion and motion control of ships and ocean structures. Norwegian University of Science and Technology, Trondheim, Norway. Lecture Notes.

Sørensen, M.E.N., Bjørne, E.S., and Breivik, M. (2016). Performance comparison of backstepping-based adaptive controllers for marine surface vessels. In *Proc. of the IEEE CCA, Buenos Aires, Argentina.*, 891–897. IEEE.